OPEN ACCESS

Impact of Testing Method on Safety Assessment of Aged Li-ion Cells: Part I – Li Plating as Main Aging Mechanism

View the article online for updates and enhancements.

Impact of Testing Method on Safety Assessment of Aged Li-ion Cells: Part I – Li Plating as Main Aging Mechanism

Gabriela G. Gerosa,[1] Max Feinauer,[1,*] Christin Hogrefe,[1] Samuel Häfele,[1] Katharina Bischof,[1] Michael Wörz,[1] Olaf Böse,[1] Margret Wohlfahrt-Mehrens,[1,2,**] Markus Hölzle,[1] and Thomas Waldmann[1,2,3,**,z]

[1]*Zentrum für Sonnenenergie- und Wasserstoff-Forschung Baden-Württemberg (ZSW), Lise-Meitner-Straße 24, 89081 Ulm, Germany*
[2]*Helmholtz Institute Ulm for Electrochemical Energy Storage (HIU), Helmholtzstraße 11, 89081 Ulm, Germany*
[3]*Institute of Surface Chemistry and Catalysis, Ulm University, Albert-Einstein-Allee 47, 89081 Ulm, Germany*

Extending the lifetime of lithium-ion batteries is essential to maximize resource efficiency and minimize environmental impact. Therefore, understanding the aging mechanisms that batteries undergo in their first life is critical to ensure safe operation in second-life applications. This study focuses on a comprehensive safety assessment of commercial 18650-type lithium-ion batteries with graphite∥NCA chemistry. The safety of aged cells with the aging mechanism of lithium plating was tested using thermal (ARC), electrical (overcurrent, overcharge, overdischarge), and mechanical (nail penetration) abuse tests. New cells without lithium plating serve as control samples for comparison of the different safety test types and for the cells with lithium plating. The presence and absence of lithium plating is confirmed by electrochemical tests and Post-Mortem analyses (SEM, GD-OES). The cells with lithium plating exhibit significantly lower onset of self-heating temperatures, a tendency to higher maximum thermal runaway temperatures and increased EUCAR hazard levels. The results highlight potential hazards associated with lithium plating in lithium-ion batteries and the necessity to detect and avoid lithium plating in first life in order to safely reuse them in second life applications. This is part one of two papers dealing with safety testing aspects of aged cells with different degradation mechanisms.

The increasing global demand for lithium-ion batteries (LIBs), driven by the growth in the number of battery electric vehicles (BEV), requires effective strategies for re-use and recycling of aged LIBs.[1,2] During usage, LIBs degrade leading to capacity loss and impedance increase. A measure defining the aging state of LIBs is the state-of-health (SOH) which can be defined as[3–5]

$$SOH = \frac{Q(t)}{Q(t=0)}100\%$$

where $Q(t)$ and $Q(t=0)$ represent the discharge capacities for the aged cell and new cell, respectively. A key avenue achieving sustainability in the LIB life cycle is to re-use batteries that have reached the end of their first life, which typically occurs when their SOH drops below 80% (see Fig. 1). These used batteries still possess valuable energy storage potential and may find a second life in less demanding stationary applications, such as stationary renewable energy storage systems.[6] Therefore, extending the life of batteries by integrating them into second-life applications is essential to maximize resource efficiency and minimize environmental impact and costs associated with LIBs on the long term.

In order to assess the ability to re-use a certain cell type, it is important to know its previous aging behavior. Understanding the aging mechanisms is a crucial step in the evaluation procedure, as it enables to ensure optimal performance and life-time, to enhance safety measures, and to effectively manage potential hazards. An aging mechanism which can lead to high aging rates[5,7–12] is the deposition of lithium metal on anodes as a competition reaction to lithium intercalation into graphite or to alloying with a silicon compound.[13] The reason for capacity fade in case of lithium metal depositions are reactions of electrolyte components on this metallic and highly reactive lithium surface[13,14] as well as formation of electrically disconnected "dead lithium."[13] Lithium deposition is thermodynamically favorable when the anode potential falls below 0 V vs Li/Li$^+$.[13,15,16] Many publications have shown that lithium deposition can occur in commercial cells and not only in pilot or laboratory LIB cells, especially at high charge rates, high end-of-charge voltages, and low temperatures.[5,7–13,16–34] Homogeneous lithium metal depositions forming during charging at low temperatures are called lithium plating.[13,35]

One approach to gain a deeper understanding of safety characteristics of cells involves conducting controlled abuse tests. These safety tests are designed to replicate safety hazards that may arise during routine operational scenarios. Depending on the nature of the failure mechanism, safety tests can be classified into three main types: mechanical (e.g. nail penetration[36–39]), electrical (e.g. overcharge,[27,37,39,40] overcurrent,[41] and overdischarge[42,43]), and thermal (e.g. overheating[37,39] and accelerating rate calorimetry (ARC)[9,11,13,25–27,36,44–49]). These tests are typically in a parameter range outside of the specifications given by the cell manufacturer's data sheets, e.g. exceeding the specified voltage window, the maximum temperature, or the maximum current. Such conditions can lead to critical conditions such as leakage, venting, fire, or thermal runaway (TR). The severity of the events caused by the abusive tests can be characterized by the EUCAR hazard levels.[50]

We have recently shown by ARC experiments that lithium plating can significantly decrease battery safety by lower onset temperature for self-heating and for TR.[9,11,25–27] In some cases, LIB cells with lithium plating showed a higher destruction level (ejection of the jelly roll) after ARC tests compared to cells without lithium plating.[11,25,51] Recently, Stottmeister and Groß showed by ab initio molecular dynamics simulations on the atomic scale that typical electrolyte molecules react exothermically with a metallic lithium surface.[14] In accordance with these simulations, Kondou et al.[52] and Fleischhammer et al.[11] showed experimentally that lithium metal also reacts exothermically with carbonate-based electrolytes. Such exothermic reactions are most likely a major cause for self-heating in ARC experiments for cells with lithium plating.[9,11,25–27,53,54]

Recently, Preger et al. identified significant gaps in the safety testing of aged cells including electrical and mechanical tests.[42] To the best of our knowledge, a comprehensive safety assessment of
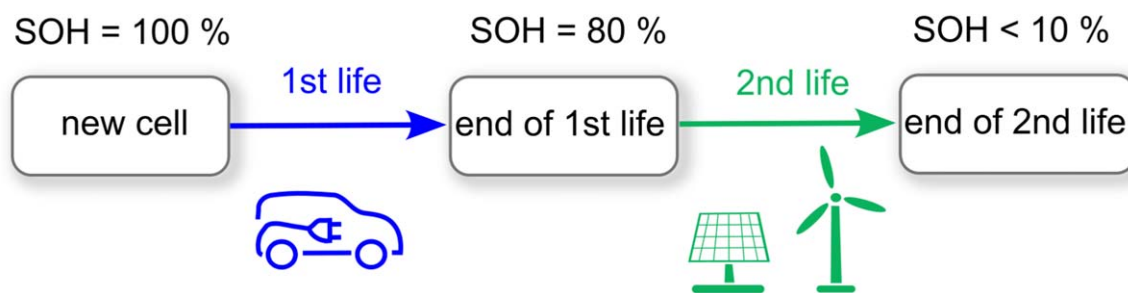
Figure 1. Concept of re-use LIBs from first life applications (e.g. BEVs) in second life applications (e.g. stationary energy storage for wind and solar energy).

aged LIBs with varying aging mechanisms has not yet been conducted. One important question therefore is, how the reactivity of cells that had undergone the aging mechanism of lithium plating affects the results of different safety testing methods.

In light of this, our research aim is to comprehensively explore the safety behavior exhibited by aged LIB cells. This work includes a detailed analysis of various abuse tests (nail penetration, overcurrent, overcharge, overdischarge, and ARC) performed on fully charged commercial 3 Ah 18650-type lithium-ion cells that have been aged at 0 °C to induce lithium plating and a comparison with the results obtained with new cells without lithium plating. The presence and absence of lithium plating in the 0 °C as well as new cells and 45 °C aged cells is supported by electrochemical evaluations and Post-Mortem analysis.

Experimental

Tested cells.—The commercial 18650-type graphite‖NCA cells used in this work had a nominal capacity of 3 Ah in a voltage range of 2.5 V to 4.2 V. The cell mass was (45.35 ± 0.13) g and the cell voltage as received was (3.55 ± 0.01) V as evaluated from 300 cells from the same batch. The cell impedance at a frequency of 1 kHz, measured with a Hioki BT 3554 battery tester, was (24.9 ± 0.2) mΩ in the fully charged state (voltage relaxed to (4.12 ± 0.03) V). The standard deviations of these values are in a similar range as for other types of commercials cells[18,55] and therefore indicate the suitability of these cells for further investigations. The technical data of the investigated cell type is summarized in Table I.

Post-mortem analysis.—Post-Mortem analysis was carried out according to our previously published workflow.[4] Cell inspection before disassembly did not show any suspicious features. The cells were discharged using five steps with different C-rates (1 C, 0.5 C, 0.25 C, 0.125 C, 0.0625 C) until 2.5 V was reached using a BaSyTec CTS battery tester. Subsequently, a new cell and a 45 °C aged cell were disassembled in a fume hood. The cell aged at 0 °C was disassembled inside an argon-filled glovebox (MBraun, $[O_2] < 0.1$ ppm, $[H_2O] < 0.1$ ppm) for safety reasons. The jelly rolls were unrolled and photos were taken from both sides of the electrodes and the separator. For further analysis, the electrodes were washed with dimethyl carbonate (DMC)[4] three times for 1 min via dip washing and then dried under vacuum conditions for 48 h at 60 °C. The electrode thickness was measured using a micrometer screw on ten

positions. Then, scanning electron microscopy (SEM) imaging (secondary electron detector, acceleration voltage: 5 kV) was conducted with a JEOL IT500 instrument. Glow discharge optical emission spectroscopy (GD-OES) analyses were performed using a GDA750 device (Spectruma) on anode samples of 2.5 mm diameter retrieved from cells aged at 0 °C and 45 °C. To prevent reactions of the atmosphere with the anodes of the 0 °C aged cells, an airtight transfer chamber was used to transfer the samples from the glovebox to the measurement device. The measurements were conducted in radio frequency (RF) mode at a frequency of 2,501 Hz, at a discharge voltage of 550 V and at a pressure of 2 hPa. A mixture of 1% H_2 in Ar (both 6.0 purity) was used as sputtering gas. The specific emission line of 670.7 nm was used for the detection of lithium. The depth profile was evaluated by our previously developed method described by Pivarníková and Flügel et al. by taking into account the intensities of the Ar 727.9 nm emission line.[56] The determination of the melting point of the separator was conducted using differential scanning calorimetry (DSC, Netzsch STA 449 C).

Electrochemical tests.—Electrochemical tests were conducted with BaSyTec CTS systems. An initial check-up cycle was performed at room temperature with each cell prior to further testing and aging. Therefore, the cells were fully charged with a constant current—constant voltage (CC-CV) protocol at a rate of 0.1 C and a cut-off current of 0.05 C in the CV phase and subsequently discharged with 0.1 C to determine the discharge capacity. For cyclic aging, the cells were placed in Vötsch climate chambers at 0 °C. Cyclic aging of the cells was performed with 0.3 C charging rate (CC-CV, 0.05 C cut-off current) and 1 C discharging rate. The aging was stopped when the cells achieved an SOH of less than 88% regarding the first discharge capacity at the aging temperature and 0.3 C. The cells were then fully charged under the same conditions as the cyclic aging was conducted to prepare the cells for the safety tests. The aged cells had a cell impedance of (29.8 ± 5.9) mΩ at (4.09 ± 0.05) V.

Besides aging at a temperature of 0 °C, additional cells were aged accordingly at 10 °C, 25 °C, 35 °C, and 45 °C. At every 50th cycle, a 0.1 C charge and discharge was conducted. The aging rate was determined from the slope of linear fits ($R^2 > 0.84$) of the SOH over cycle data, excluding the cycles at 0.1 C.

ARC tests.—An ARC-ES from Thermal Hazard Technology (THT, UK) with radiant heater was used for the ARC measurements. The fully charged cells were prepared for the ARC test by removing the shrink tube and electrically insulating the positive tab with a polyamide tape. The cell, together with a type-N thermocouple on the cell surface, was then fixed in a thin steel sheet to mount the cell free hanging on the top of the ARC reaction vessel. A calibration and drift test of the ARC system with an empty 18650 cell can ensured the correct heating rate of the ARC device to provide quasi adiabatic conditions. A heat-wait-seek (HWS) program was used during the ARC experiments to investigate the critical temperatures. Starting from 35 °C, the temperature was increased in steps of 5 °C, followed by a 15 min rest period for temperature homogenization/stabilization. During the subsequent 10 min seek period, the temperature

Table I. Technical data of the investigated graphite‖NCA cell in this study provided by the manufacturer.

Parameter	Value
Nominal capacity (at 0.2 C discharge)	3 Ah
Max. charge voltage	4.20 V
Min. discharge voltage	2.50 V
Average working voltage (at 0.2 C)	3.65 V
Max. charge rate (at RT)	0.55 C
Max. discharge rate (at RT)	2.0 C
Temperature range during charging	0 °C–45 °C

change was measured. If the temperature rate exceeded the exothermic sensitivity of $0.02\,°C\,min^{-1}$, the reaction was defined as exothermic, no further heating steps were performed, and the calorimeter simply followed the cell temperature. As the cell temperature increased and exothermic reactions were ongoing in the cell, the gas pressure within the cell increased, resulting in cell venting. Finally, the cells went into TR, which was defined by a sudden increase in the self-heating rate (SHR) and ended with the cell explosion. The ARC tests were stopped by cooling with pressurized air when the cell temperature exceeded 350 °C. The ARC tests were conducted with two new and two aged cells.

Electrical abuse tests.—A cell tester (Digatron UBT 150-020-3 RE) was used to perform the overcharge, overdischarge, and overcurrent abuse tests. Temperature sensors were attached to the positive terminal, to the negative terminal, and to the center of the cell container.

For the overcharge tests, the fully charged cells were charged at a constant current rate of 1 C until 200% SOC was reached or an off-nominal event occurred (such as TR). Overdischarge tests were commenced on fully charged cells by CC discharging at 1 C until −150% SOC (end criterion) was reached or an off-nominal event occurred. During the overcurrent tests, the cells underwent continuous cycling, CC charging at 1.1 C until reaching 4.2 V and CC discharging at 4 C until reaching 2.5 V, without pause. The end criterion was 100 cycles or the occurrence of an off-nominal event. If 100 cycles were conducted without exhibiting out-of-specification performance characteristics, an additional capacity check at a 0.2 C charging rate (CC-CV, 0.02 C cut-off current) and 0.2 C (CC) discharging rate was performed.

The overcharge and overdischarge tests were each conducted with three new and three aged cells. The overcurrent cycling tests were conducted with three new and four aged cells.

Nail penetration tests.—The nail penetration tests on fully charged cells were performed in a dedicated explosion-proof bunker at ZSW (open system in view of pressure). Exhaust gases were cleaned in a three stage exhaust purification system. The nail speed and force were controlled by linear drive (penetration speed of $0.1\,mm\,s^{-1}$ and force up to 1 kN). A ceramic nail (ZrO_2, Ø 3 mm, tip angle = 45°) was fully penetrated into the cell. The nail remained inside the cell during the subsequent TR. The temperature sensors were attached similar to the electrical abuse tests to the positive terminal, the negative terminal, and to the surface shell. The nail penetration tests were performed with two new and two aged cells.

Results and Discussion

Characterization of lithium plating after aging.—Figure 2 shows photographs of unrolled anodes and cathodes from disassembled 18650 cells. The anodes from new cells (Fig. 2a) and cells cycling aged at 45 °C (Fig. 2b) look similar on visual inspection. In contrast, the anode from a cell cycling aged at 0 °C looks grey (Fig. 2c), which was also observed before in other types of LIBs cycled at low temperature with homogeneous lithium plating.[13,25,35,57] The cathode colors appear very similar for all three cells Figs. 2a–2c.

The anode and cathode parts that were on the inside of the jelly roll of the aged cells show characteristic kinks (right hand side of Figs. 2b, 2c), whereas electrodes from new cells do not exhibit those (Fig. 2a). These deformations of the inner part of the jelly roll are in agreement with other types of cyclically aged cylindrical LIB cells showing jelly roll deformations in X-ray computed tomography and metallographic cross-sections.[58–61]

Figures 3a–3c show SEM measurements of the electrode surfaces. The anode from the new cell shows flaky graphite without deposits (Fig. 3a). After aging at 45 °C (Fig. 3b), depositions on the graphite particles are observed. However, the overall electrode morphology from the new cells is still visible after aging at 45 °C.

In contrast, after aging at 0 °C, the graphite particles on the anode surface are covered by a thick film. This is in accordance with other cell types cycled at low temperatures.[25,62] Both, the anode of the 45 °C aged cell and the 0 °C aged cell exhibit an increase of the thickness on each side of the coating of 9 μm and 8 μm, respectively (Table II), indicating microstructural changes and deposition processes in both cells. As for other cell types, these results show that the aging mechanisms on the anode are different for both 0 °C and 45 °C.[5,7–10,13,25,26,63]

On the cathode surface, no clear differences between the new cell, the 45 °C aged, and the 0 °C aged cells can be seen (Figs. 3a–3c). This is consistent with graphite and Si/graphite anodes from other cell types, where the primary aging effects are often found rather on the anode than in the cathode.[5,30,64]

Using GD-OES depth profiling, the elemental distribution of lithium in the aged anodes was analyzed within the top 20 μm of the electrodes (Fig. 3d). For the 45 °C aged cells, a small lithium peak was observed at the very anode surface and with increasing depth, the lithium concentration is constant. This small lithium peak on the anode surface is likely due to the aging mechanism of SEI growth and shows the absence of lithium plating, as observed for other cell types.[25,30] In contrast, a significantly higher lithium concentration can be found on the anode surface of the 0 °C aged cells. This lithium peak has a maximum of ~18 wt% and is much broader compared to the one of the 45 °C aged anodes, indicating lithium plating on the anode surfaces of the low temperature cycled cells.[18,19,25,62,65]

The presence of lithium plating for the cells cycled at 0 °C is supported by:

1) Low Coulombic efficiency (CE) of 97% during aging. A low CE-value does not directly indicate lithium plating but strong side reactions as a consequence of lithium plating.[12] In case of lithium plating such side reactions are likely the reaction of deposited lithium metal with electrolyte[13,14] and formation of electrically disconnected "dead lithium."[13] In contrast, the CE of the cells aged at 45 °C was higher than 99.9%.

2) The capacity fade (Fig. 4a) and aging rate (Fig. 4b) at 0 °C is much higher compared to 25 °C, which is a strong indication of lithium plating.[5,7–9,13,35,63] The cells aged at 0 °C reached 80% SOH in average after only 29 cycles. In contrast, for aging at 25 °C and 45 °C cells reached 80% SOH after 659 cycles and 384 cycles in average, respectively. The Arrhenius-plot of the cyclic aging rates in Fig. 4b exhibits a V-shape, which was also found in other aging studies[5,7–10] and simulations.[63] In those previous studies, the high temperature branch (left hand side of the minimum, 25 °C–45 °C) exhibited the aging mechanism of accelerated solid electrolyte interphase (SEI)-growth, whereas the low temperature branch (right hand side of the minimum, 25 °C–0 °C) exhibited lithium metal plating as main aging mechanism.[5,7–10,63] The aging rate minimum in the Arrhenius plot typically gives the transition temperature at which the main aging mechanism is changing.[5,7–10,63] In the investigated cells, the minimum is found at 25 °C. Cell disassembly of cells aged at 0 °C and 45 °C confirmed these indications for the main aging mechanisms in the cells in this study (compare Figs. 2 and 3).

3) The shoulder at the beginning of the voltage discharge curve after charging at 0 °C indicates stripping of previously plated lithium metal (see arrow in Fig. 4c).[13,23,25,66] Cells cycled at 25 °C and 45 °C did not exhibit such a voltage plateau.

4) A film on the anode of the 0 °C aged cell. This film on the anode surface is visible in photographs (Fig. 2c), SEM measurements (Fig. 3c), GD-OES measurements (Fig. 3d). This is in contrast with the 45 °C aged cells.

These observations by Post-Mortem analysis and electrochemical tests indicate that lithium plating is present in the 0 °C cycled cells. New cells that are used as control samples in this paper, do not exhibit any lithium metal plating. The presence of lithium plating in

Figure 2. Photographs of unrolled anodes and cathodes from disassembled 18650 cells. (a) new cell, (b) 45 °C aged cell, (c) 0 °C aged cell. The electrode parts that were inside the jelly rolls are on the right hand side.

different commercial cells and cells built on pilot-scale after cycling at low temperature is consistent with many observations by different researchers.[5,7–13,16–34] In contrast, the 45 °C cycling aged cells with a similar SOH do not show lithium plating since their degradation is due to a different main aging mechanism, most likely SEI growth.

The safety behavior of the cells aged at 0 °C with lithium plating compared to new cells without lithium plating is discussed in the following sections of the present work.

Accelerating rate calorimetry.—ARC tests were performed to determine critical temperatures and to evaluate the safety behavior of cells without and with lithium plating (Fig. 5). ARC experiments represent an extreme case, where no heat can dissipate from the cells, i.e. quasi-adiabatic conditions or thermally perfectly insolated cells. The SHR is displayed in Fig. 5b, illustrating the derivation by time of the exothermic part in the curves represented in Fig. 5a.

The significant events during the ARC tests are depicted in Fig. 5. First, the ARC device heats up the LIB sample in steps of 5 °C until a significant SHR is detected (T_{SH} for SHR > 0.02 °C min^{-1}). The venting of the cells is marked in Fig. 5a as it can be seen by the temperature drop in each temperature curve at T_{vent} due to the rapid venting of gas which can be described by the Joule-Thomson effect. The TR temperature T_{TR} is defined as the temperature where a significant jump of the SHR is detected, typically around 100 °C min^{-1}. Finally, the cell reaches its maximum temperature T_{max} followed by cooling down after the reactions utilizing the available chemical and electrochemical energy in the cells reached completion. The reproducibility of the new and aged cells regarding T_{SH}, T_{TR}, T_{vent} was in a similar range as observed before.[9,11,13,25–27]

Both tested 0 °C aged cells with lithium plating showed significantly lower T_{SH} values of ~35 °C, compared to new cells without lithium plating ($T_{SH} \approx$ 80 °C). Furthermore, the aged cells with lithium plating showed a higher SHR during the test (Fig. 5b). These results are in accordance with earlier ARC results with different 18650 cell types with and without lithium plating.[11,25–27]

Venting occurred in the range of 121 °C and 133 °C for one of the aged and the two new cells. The similarity of the venting temperature was also observed in ARC tests with other cell types

without and with lithium plating.[9,27] One of the aged cells did not show a temperature drop during venting, which is similar to other types of 18650 cells with lithium plating in ARC tests.[25] In such cases, the SHR is likely too high to observe the temperature drop, however for other cells simultaneous audio recordings had shown that venting can still occur.[25]

The ARC test time to TR as measured with different cells in our group has been observed to show a tendency to be shorter for cells with lithium plating,[25–27] which is also the case in the present study. All cells tested had similar T_{TR} temperatures of ~203 °C regardless of the presence of lithium plating on the anodes. While this is in accordance with ARC tests of another pouch cell type,[9] other 18650 cells showed a more[25,26] or less[27] clear tendency to lower T_{TR} temperatures. Both aged cells with lithium plating showed higher maximum temperatures T_{max} of ~650 °C, compared to new cells without lithium plating with almost 100 °C lower maximum temperatures. In contrast, other cell types with lithium plating on the anodes showed similar or slightly lower T_{max} values in ARC tests.[25–27]

In summary, the presence of lithium plating in the tested cell type resulted in a significant decrease in safety properties in ARC tests, as evidenced by the lower T_{SH}, higher SHR, shorter time until TR, and higher T_{max}, while other values (T_{vent}, T_{TR}) are similar to cells without lithium plating. We would like to point out that the reason for the TR of the cells with lithium plating in the ARC experiments are exothermic reactions of lithium metal with electrolyte[9,11,13,14,25–27,53] and not internal short circuits caused by lithium dendrites.[13,67]

Overcharge.—Electrical abuse testing in LIBs involves intentionally exceeding the voltage and current limits specified by the cell manufacturer. During normal operation in many applications, the battery management system (BMS) monitors compliance with voltage, current, and temperature limits. However, e.g. a failure of the BMS or external electrical factors that act on the cell and deviate from normal conditions, can increase the risk to overcharge, excessive heat generation, internal short circuits, and thus could even cause TR of the battery.
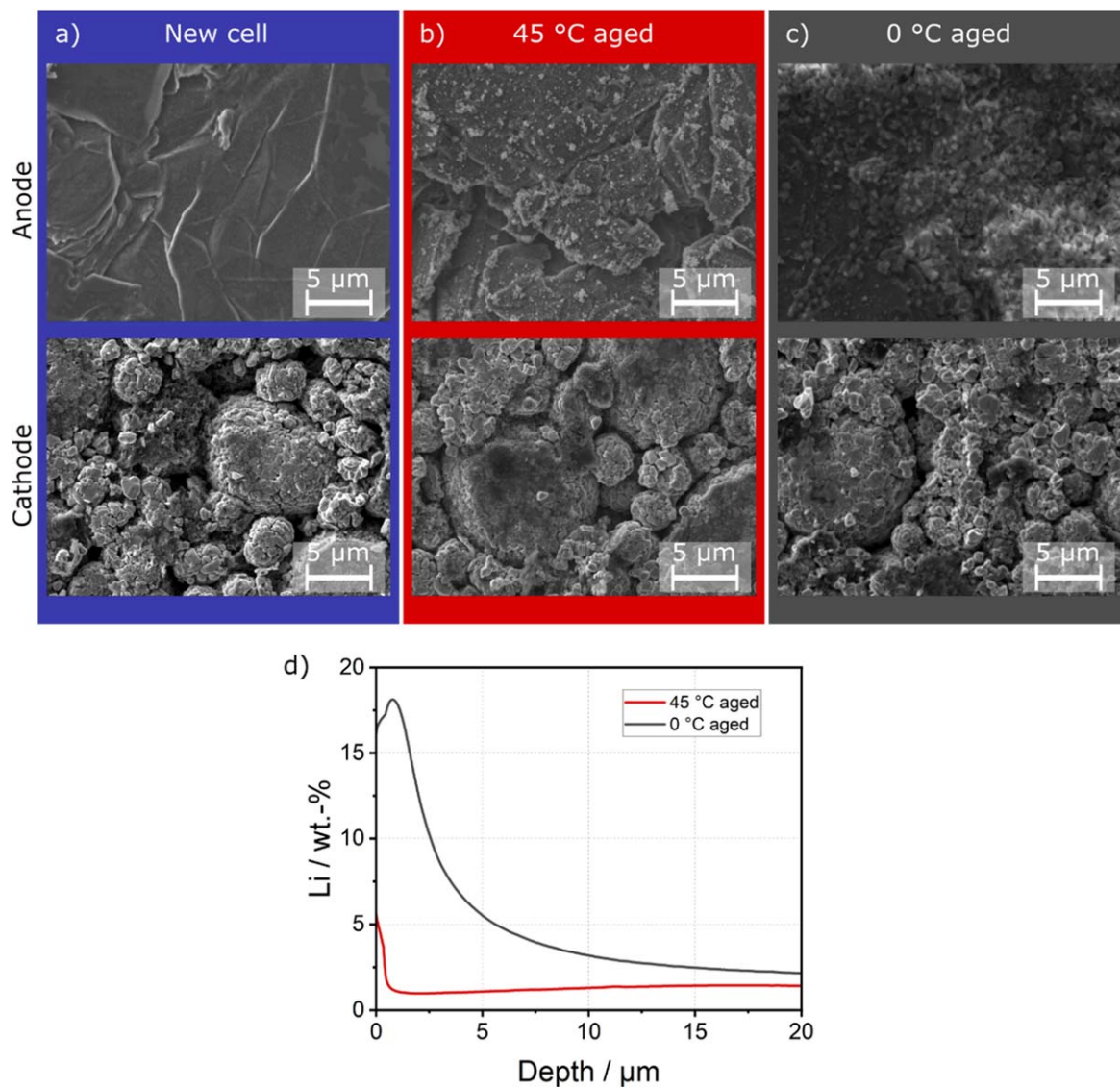
Figure 3. Top view SEM image of the anode (upper images) and cathode (lower images) for (a) the new cell, (b) the 45 °C aged cell, (c) the 0 °C aged cell. (d) GD-OES depth profile of the 45 °C aged (red) and the 0 °C aged (grey) anode, showing the lithium concentration within the top 20 μm of the electrodes.

Table II. Electrode thicknesses (double-side coated) after cell disassembly for the new cell, 45 °C aged cell, and 0 °C aged cell.

	new	45 °C aged	0 °C aged
Anode thickness/μm	174	192	189
Cathode thickness/μm	136	137	132

Overcharge tests were performed to evaluate the safety performance of these cells when charged to voltages above the specification. The manufacturer's specified voltage range for the commercial 18650 type NCA‖graphite cells is 2.5 V to 4.2 V. Therefore, any charging operation exceeding the upper limit of 4.2 V represents an overcharge condition. The purpose of the manufacturer's upper limit is to prevent excessive release of lithium ions from the cathode which leads to critically high cathode and critically low anode potentials.[68] If the cathode potential exceeds the stability window of the electrolyte, side reactions such as gas formation will occur.[69,70] Additionally, during overcharge, the anode potential will decrease.[71] If the anode potential decreases below 0 V vs Li/Li$^+$, lithium deposition

on the anode becomes thermodynamically favorable.[13,15,16] Lithium deposition can therefore even occur in the new cells during overcharge. In the aged cells, where lithium plating was already present it is likely that additional lithium is deposited on top.[27] The already existing lithium plating might provide crystallization nuclei and foster further lithium deposition. Therefore, it can be expected that the aged cells with lithium plating react differently in overcharge tests when compared to cells without lithium plating.

Figure 6a shows the temperature curves of new cells without lithium plating and aged cells with lithium plating during overcharge tests. The three new cells reached their maximum temperatures below 97 °C. In contrast, the three aged cells exhibited their maximum temperatures in the range of 105 °C to 169 °C. While two cells showed only severe heating, the cell with the highest temperature observed a TR resulting in disintegration of the cell. These outcomes are most likely due to the presence of more lithium plating on the anodes of the aged cells in the overcharge test, resulting in increased exothermic side reactions between lithium plating and the electrolyte.[13,14,25–27,53]

The cell voltage profiles of new and aged cells during the overcharge tests are shown in Fig. 6b. In the case of all three tested
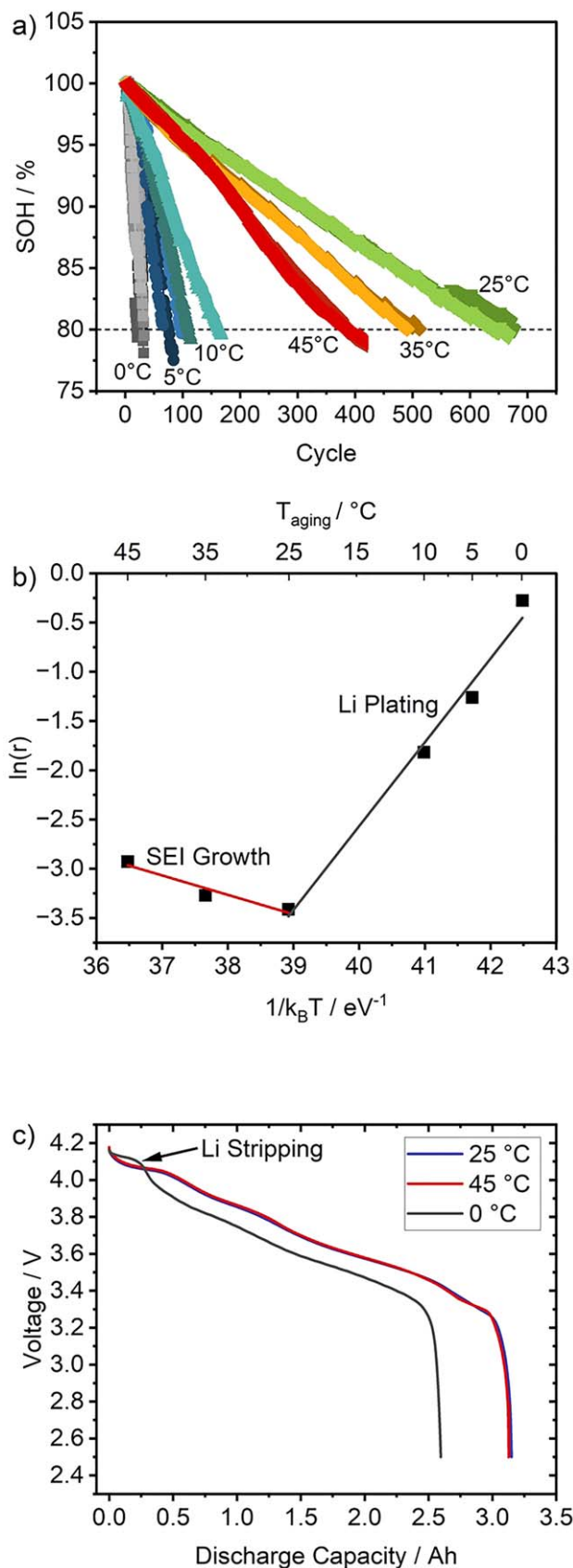
Figure 4. (a) SOH decline over cycles for 18650 cells cycled with 0.3 C charge/discharge at different temperatures. (b) Arrhenius-plot, which was determined by the slopes in a). (c) Discharge cell voltage curves voltage of the first cycle (charge: 0.3 C, discharge: 0.1 C) at 25 °C (blue line), 45 °C (red line), and 0 °C (dark grey line). The arrow marks the voltage shoulder for the discharge after charging at 0 °C, which indicates lithium stripping.

new cells, the voltages profiles initially reached a peak value of ~5.25 V and subsequently exhibited a gradual decline to ~4.8 V. Remarkably, this voltage level of around 4.8 V was maintained for a duration of almost 5 min, even during further charging. Similar voltage maxima were observed in the voltage profiles for graphite‖LCO cylindrical cells[72] and prismatic graphite‖NMC111 cells.[73] By ICP[72] and XRD[73] analysis at different overcharged states, both studies found that the maximum coincided with a fully delithiated cathode, leading to insufficient Li-ion extraction, extensive electrolyte decomposition, and heat release. In Fig. 6b, the maximum of both new cells and aged cells coincides with a more severe heat release (compare Fig. 6a).

For the aged cells, the lithium inventory in the cathode is typically reduced due to reactions of the lithium depositions on the anode surface. Therefore, one might expect an earlier appearance of the maximum in the aged cells. However, this was not observed as can be seen from Fig. 6b. Another explanation of the very different voltage profiles could be usage of overcharge additives in the electrolyte, such as biphenyl or cyclohexyl benzene, which can be found in LIB cells.[28,68,74] The working mechanism of such additives is to polymerize during overcharge in order to form a protective film on the cathode surface, while keeping the voltage at a constant level.[74] For some additives, this leads to gas formation, which might cause the CID to be triggered earlier.[68,75] However, for example biphenyl was found to be decomposing during aging.[28] Electrolyte investigation was out of scope of the present paper, however, if similar additives were used in the commercial cells in the present paper, it might explain the different voltage profiles for new and aged cell.

The voltage is interrupted for the new cells at SOCs of 123%, 126%, and 124%. The aged cells showed a delayed voltage interruption at SOC values of 166%, 162%, and 164%. The voltage interruption might have been caused either by CID triggering (due to gas generation by side reactions[27]) or shut down of the separator (due to high temperature[76]).

The onset and maximum temperatures recorded in DSC measurements—136 °C and 141 °C—showed that the examined LIBs feature most likely a polyethylene (PE) separator, which melts in the range of 120–140 °C.[76] These temperatures are not reached on the cell surface for the three new cells and for two of the aged cells. Only for one of the aged cells the temperature on the cell surface exceeds this temperature range.

Higher maximum temperatures (>500 °C) were observed in overcharge tests of 60 Ah pouch (graphite‖NMC),[37] 60 Ah prismatic (graphite‖NMC),[37] and 50 Ah prismatic cells (graphite‖NMC811).[39] Lamb et al. showed that the enthalpy of TR increases with cell capacity,[45] therefore it is not surprising that larger cells show higher T_{max} values during overcharge than the cells investigated in the present study.

It is important to note that the internal temperature in cylindrical cells typically exceeds the temperature on the cell surface. One reason is cell heating due to discharge current.[77–80] However, for a 1 C discharge, the maximum temperature difference between cell surface and cell core was observed to be only ~5 °C for another 18650 cell type.[77] Although the temperature gradient in cylindrical cells depends on the tab design[79,81] and electrode/separator thicknesses,[82] it is reasonable to expect a contribution in a similar order of magnitude for a 1 C overcharge for the tests performed in this paper.

Another contribution for cell heating during overcharge is reaction heat, which can also increase the internal temperature and cause separator melting. We had recently equipped cylindrical 21700 type cells with internal temperature sensors during ARC tests.[49] In those experiments, the maximum temperatures were ~600 °C and ~1000 °C on the cell surface and inside the jelly roll, respectively, which is an increase by 67%.[49] In the present study, a rough estimation leads to ~161 °C for the internal cell temperature, if we take $T_{max} = 97$ °C on the cell surface with an increase by 67% into account. 161 °C is above the melting temperature range
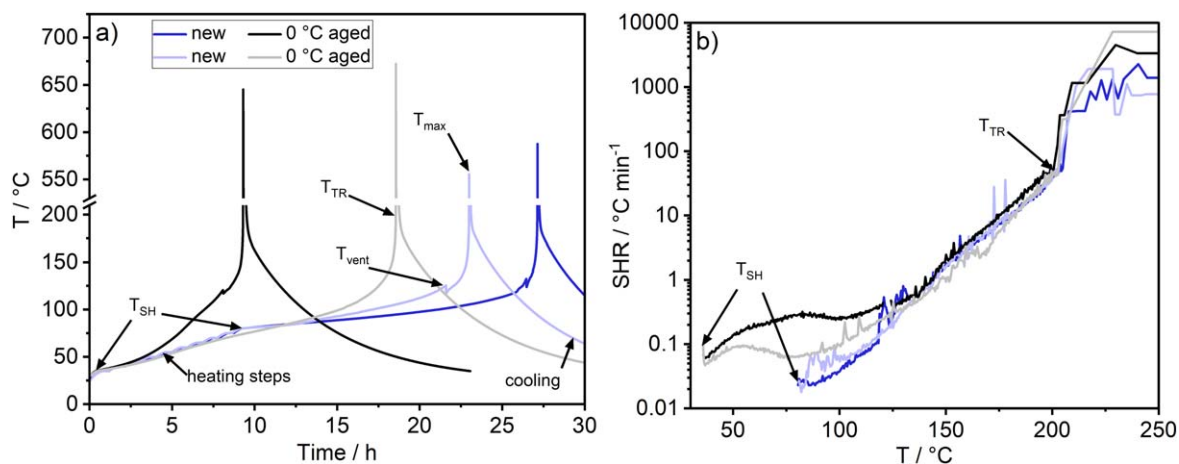
Figure 5. ARC test results for fully charged new cells without lithium plating (light and dark blue) and aged cells with lithium plating (black and grey). (a) Temperature curves as a function of test time. (b) SHR as a function of temperature. The temperatures were recorded at mid-height of the 18650 cell cases.
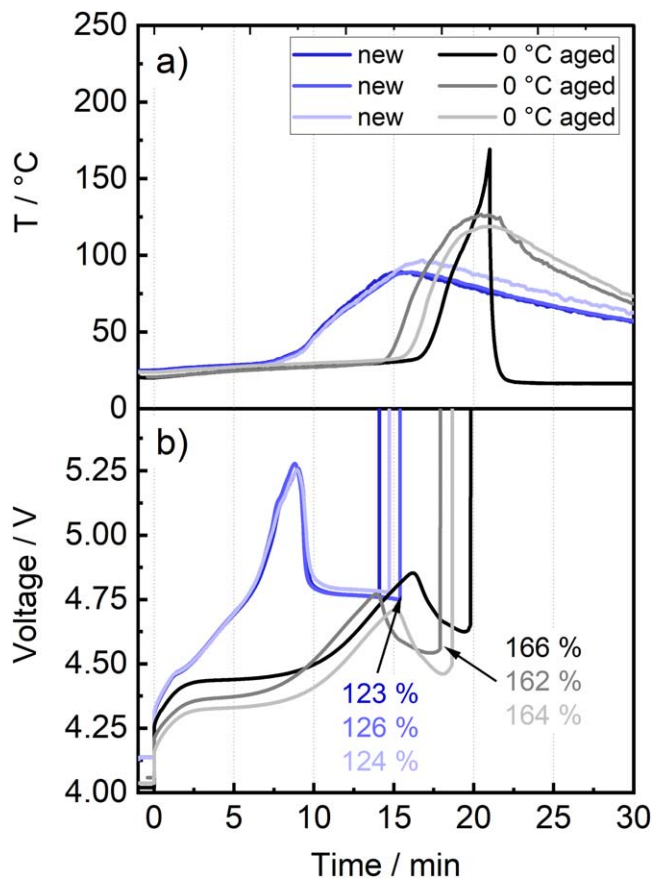

Figure 6. Overcharge test results of fully charged new cells without lithium plating and aged cells with lithium plating. (a) Temperature curves (highest observed temperature on the cell housing) and (b) cell voltage profiles. The SOC of the cells at the time of CID triggering is highlighted. The SOC is calculated based on the nominal capacity for new cells and the remaining capacity for aged cells.

(120 °C–140 °C)[76] of the PE separator. Therefore, the voltage break which happens near T_{max}, could have also been caused by separator melting. However, this is unlikely since separator melting would most likely not lead to an abrupt voltage change. Therefore it is more likely that the voltage interruption is rather caused by CID opening.

For all tested cells, only one 0 °C aged showed a more severe reaction close to a TR. Another 0 °C aged cell exhibited extensive

expansion during overcharge, while the third did not exhibit any optical changes. In contrast, the new cells only exhibited CID opening during the overcharge test.

The ARC experiments in the present work lead to higher T_{max} during TR for both new and aged cells. The trend of higher T_{max} for the aged cells with lithium plating is similar for both, the ARC and the overcharge tests. In contrast to previous overcharge experiments in ARC,[27] the conditions were not quasi-adiabatic in the overcharge experiments of the present study, i.e. heat was able to be dissipated. Both studies use cells with the same format (18650), as well as a similar cell chemistry (graphite‖NCA) and cell capacity (3.25 Ah[27]/3 Ah). In our previous ARC study,[27] the T_{max} values were in a range which is more similar to the T_{max} values of the ARC tests in the present study. Therefore, it is likely that the higher temperatures in the ARC experiments in the present work are due to the quasi-adiabatic conditions.

In summary, the new cells did not contain lithium plating before the experiment, however lithium is likely to be deposited during overcharge because of anode potentials below 0 V vs Li/Li$^+$. In contrast, in the aged cells lithium plating was already present before experiments and additional reactive lithium is most likely deposited on top of it. The higher amount of lithium deposition in the aged cells leads most likely to increased heat generation from exothermic reactions with electrolyte[9,11,13,14,25–27,53] and consequently to the higher observed T_{max} values.

Overdischarge.—Overdischarge occurs when a cell is discharged below the voltage level recommended by the cell manufacturer. For the cells tested in this study, overdischarge begins for cell voltages below 2.5 V. Overdischarge can happen for instance due to failure of the BMS or due to long-term self-discharge during storage particularly at low state-of-charge (SOC). Some of the consequences of overdischarge are the decomposition of the SEI leading to gas release and dissolution of the copper current collector (forming most likely Cu$^+$ ions)[83] from the anode and deposition on the cathode, separator, and anode surface.[83–87]

Figure 7a shows the temperature curves of new cells without lithium plating and aged cells with lithium plating during overdischarge tests. All three new cells reached their maximum temperature at approximately 64 °C. In contrast, the aged cells exhibited slightly higher maximum temperatures at 80 °C, 74 °C, and 76 °C, respectively. In addition, the aged cells reached their temperature peaks earlier than the new cells, indicating a less safe behavior of the aged cells with lithium plating.

Fear et al. overdischarged new 18650 cells with a similar capacity (3.35 Ah) and chemistry (graphite‖NCA).[43] Therefore, they are to some extend comparable to the present work. The maximum temperatures[43] of ~80 °C were in a similar range as for
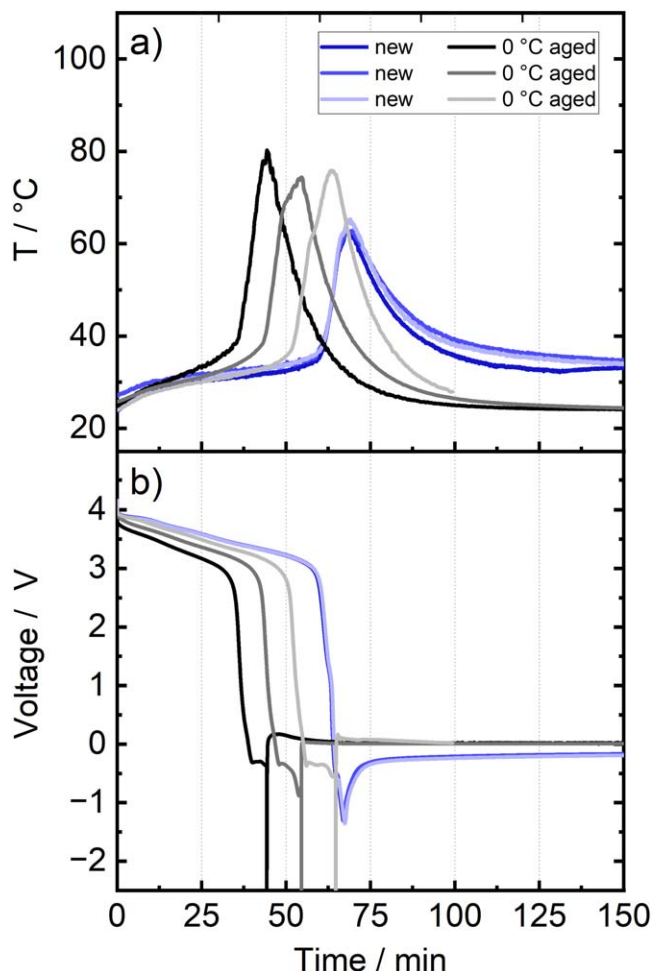
Figure 7. Overdischarge test results of fully charged new cells without lithium plating and for aged cells with lithium plating. (a) Temperature curves (highest observed temperature on the cell housing) and (b) cell voltage profiles.

the cells in the present study. Please note that Fear et al. overcharged new cells,[43] however, their maximum temperatures are more in the range of the aged cells with lithium plating of our study. Therefore, the temperature increase due to lithium plating in overcharge experiments in our study can most likely be regarded as non-critical.

Figure 7b displays the cell voltage profiles during the overdischarge tests. Initially, all cells experienced normal discharging within the manufacturer's recommended voltage range of 4.2 V to 2.5 V. Below the end-of-discharge voltage of 2.5 V, overdischarge and cell reversal (below 0 V, also called extreme overdischarge)[18] was induced, causing the cells to reach their minimum voltage levels of −1.3 V for new cells and approximately −0.3 V for aged cells. Subsequently, the voltage levels of new cells increased slightly to −0.2 V and remained constant until the end criterion (−150% SOC) without activation of their CIDs.

In summary, the experiments on overdischarge for the aged cells with lithium plating showed slightly higher T_{max} values compared with the new cells without lithium plating. This is similar as in the ARC and overcharge experiments and is likely caused by exothermic reactions of the deposited lithium with electrolyte.[9,11,13,14,25–27,53] The temperature difference between the new and aged cells is not as pronounced for overdischarge as for overcharge, since deposited lithium can be stripped during the overdischarge, whereas more lithium is deposited during overcharge.

Overcurrent cycling.—The purpose of overcurrent cycling is to evaluate a cell's safety performance under repeated high-current discharge and charge conditions. In applications, overcurrents can for example be caused by a defective BMS.

Figure 8a shows the temperatures during the overcurrent tests with new cells without lithium plating and with aged cells with lithium plating. The applied C-rates were chosen to be twice as high as the maximum allowed charging C-rate in the cell product data sheet.

In all three new cells, T_{max} was below 87 °C in the first discharge and well reproducible. However, as the aged cells with lithium plating showed large deviations in the safety behavior, a fourth overcurrent cycling test was conducted. Two of the aged cells reached T_{max} values of 122 °C and 141 °C and only exhibited venting, while two other aged cells experienced a TR with corresponding maximum temperatures above 450 °C. Figure 8b shows the corresponding cell voltages. It can be seen that the safety critical event happens at the end of the discharging step in all four aged cells with lithium plating.

The TR of two of the aged cells is attributed to a ~20% higher average cell impedance of the aged cells with lithium plating compared with the new cells without lithium plating. In addition, the aged cells produce most likely a larger amount of gas due to the reacting lithium plating with electrolyte. As a result, the four aged cells exhibited CID activation after only one overcurrent discharge. In contrast, the new cells were able to perform 100 overcurrent cycles (4 C discharge, 1.1 C charge). After the overcurrent testing, an additional capacity check at 0.2 C was conducted in order to determine the capacity loss. The new cells reached a discharge capacity of 2.4 Ah in this test, which corresponds to 80% of the initial capacity of 3 Ah at 0.2 C.

From the ARC experiments and from literature[9,11,25–27] it is known that cells with lithium plating exhibit exothermic reactions at comparably low onset temperatures. In the overcurrent tests, the heating due to current flow at high C-rates[55,77–80,82] in combination with slow heat dissipation and exothermic reactions seems to be sufficient to force two of the four aged cells with lithium plating into TR. The fact that two of the aged cells did not show a TR although they were very similar to cells with TR suggests a statistical behavior. However, a statistical evaluation would require a larger number of tests, which is out of scope of the present study.

In summary, the overcurrent cycling tests showed that the aged cells with lithium plating were only able to perform one single discharge step, whereas the new cells without lithium plating could still perform 100 cycles. Furthermore, two of the aged cells went into TR, by contrast to the new cells. The reason for the failure are most likely exothermic reactions of the deposited lithium with electrolyte[9,11,13,14,25–27,53] in combination with cell heating due to current flow where it is known that higher C-rates lead to higher maximum temperatures.[55,77–80,82] Especially inside the cells, the temperatures are typically higher than on the cell surface.[49,77–80]

Nail penetration.—Mechanical damage to battery cells can potentially cause internal short circuits. Mechanical abuse testing serves as a valuable tool for testing real-world failures under well controlled conditions and is of particular importance in the electric transportation industry, where safety risks to in-use batteries are posed by crash and impact scenarios.[88] Among the various safety tests, nail penetration is one of the most commonly used methods.

The temperature curves observed during the nail penetration tests are shown in Fig. 9a. It is noteworthy that two of three aged cells, exhibited an earlier onset of temperature rise compared to the three new cells. However, the average maximum temperatures reached by both the new cells (624 °C) and aged cells (618 °C) were similar. This finding aligns with the observations from Friesen et al., who also noted that fully charged commercial 18650-type lithium-ion cells reached comparable temperatures during nail penetration tests of both new cells without lithium plating and aged cells with lithium plating.[89]

Similar maximum temperatures (>596 °C) were also observed by Ohneseit et al. for nail penetration tests with four different types of
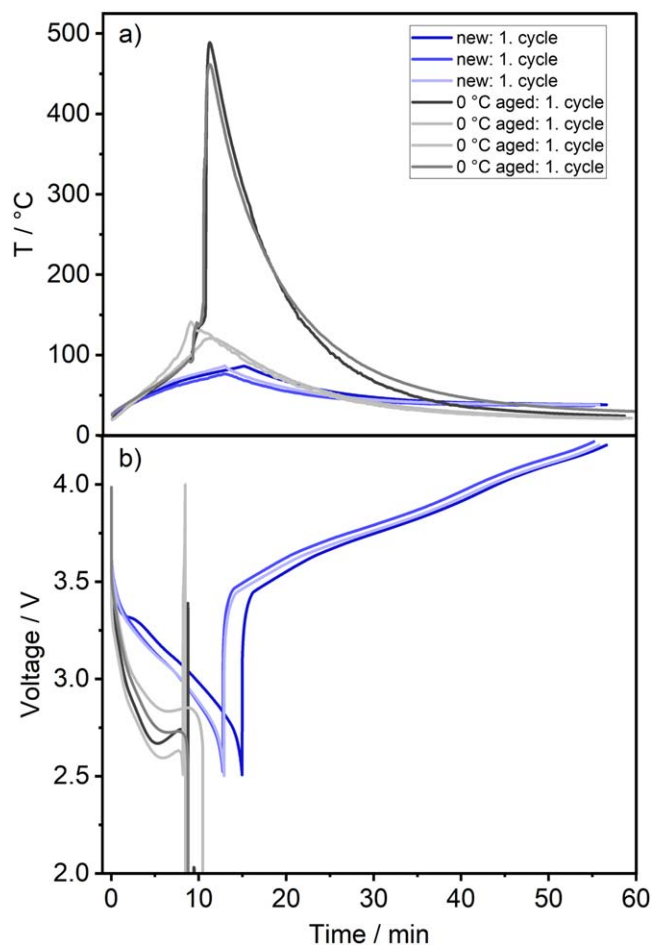
Figure 8. (a) Temperature curves of the first cycle of the new cells without lithium plating and aged cells with lithium plating during overcurrent cycling tests. (b) Cell voltage of the first cycle of the new cells and the aged cells.
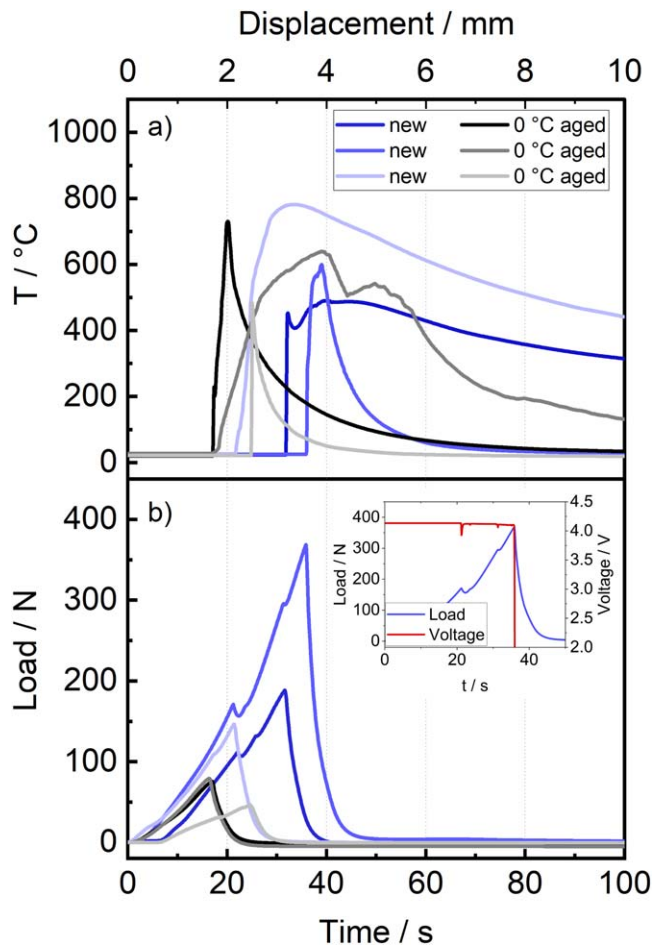

Figure 9. Nail penetration test results of fully charged new cells without lithium plating and aged cells with lithium plating. (a) Temperature curves (highest observed temperature on the cell housing) and (b) load curves. The inset in (b) exemplarily shows the agreement of the cell voltage drop and the load maximum for one new cell.

21700 cells with graphite+Si anodes and NMC811 and NCA cathodes with capacities in the range of 4–5 Ah.[36] Higher T_{max} values were observed in nail penetration tests of 60 Ah pouch ($\sim$800 °C),[37] 60 Ah prismatic ($\sim$800 °C),[37] and 50 Ah prismatic cells ($\sim$600–700 °C),[39] as these cells were significantly larger. T_{max} was lower ($\sim$100 °C) for 3 Ah 21700 cells with graphite∥LFP electrodes, which is most likely caused by the lower energy content due to the LFP cathodes.[36] Lamb et al. also observed lower T_{max} values for LFP cells compared with NCA cells in ARC tests, even if the LFP cells had higher cell capacities.[45] Therefore, it seems that, in nail penetration tests, T_{max} depends on both the cell chemistry, capacity, and form factor.

Figure 9b shows the mechanical load curves obtained during nail penetration tests for both, new cells without lithium plating and aged cells with lithium plating. Especially the new cells exhibit load drops, which coincide with voltage drops, indicating soft short circuits (see inset of Fig. 9b).[38] The peak points mark the onset of internal fracture and hard short circuit.[38,90] Notably, new cells reached a higher load exceeding 146 N, in contrast to aged cells with values below 80 N. In fact, the aged cells showed lower values than the forces needed to induce the soft shorts in the new cells. This discrepancy highlights that cells with lithium plating exhibit significantly different mechanical properties. This phenomenon might be explained by higher internal cell pressure. Willenberg et al. observed a pressure increase in aged cylindrical cells by continuously growing layers on the anode.[91] Such a layer could be lithium plating, since lithium is known to deposit mostly on the anode surface.[15,25,62] For pouch cells with lithium plating, different groups observed an increase of cell thickness due to thicker anodes.[57,92,93] In contrast, in cylindrical cells with rigid housing,

an increased anode thickness translates to increased pressure which could affect the penetration of the nail. An additional contribution to the increase of internal pressure could originate from gas generation during aging.[94–96]

In summary, the results of the nail penetration experiments showed that the aged cells with lithium plating behaved similar as the new cells without lithium plating regarding the measured maximum temperatures. Most likely, the internal short circuits generated by the nail are so severe that the presence of lithium plating makes no large difference. However, we found the mechanical integrity of the 0 °C aged cells to be changed, i.e. less force is needed to penetrate and short circuit the cells with lithium plating, making them less save in terms of deformation.

Comparison of results from different types of safety tests on cells with and without lithium plating.—A comprehensive comparison of the safety test types and results between new cells without lithium plating and aged cells with lithium plating is made in the following. Figure 10a provides the maximum temperatures reached during all safety tests conducted in the present work. When analyzing the maximum temperature, it is always important to keep in mind that it is subject to some variation, as even small differences in the TR process can cause large variations in the measured maximum temperature. In this light, the results show some scattering, however, the evaluation reveals clear trends.

In both, ARC and overcharge experiments, aged cells with lithium plating consistently showed slightly higher maximum
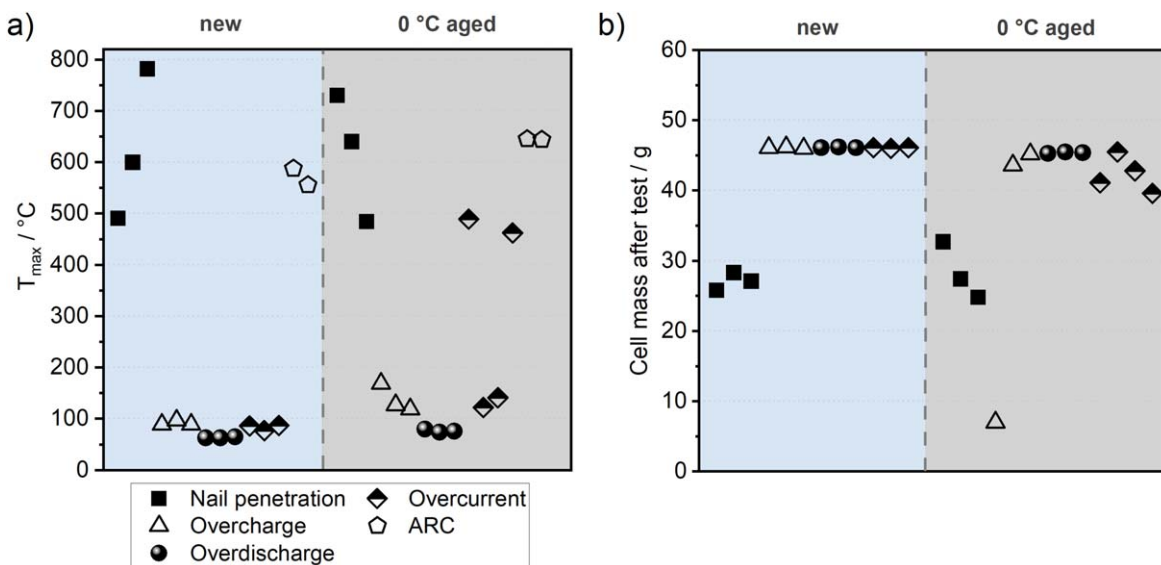
Figure 10. Comparison of (a) maximum temperatures during abuse testing and (b) cell masses after abuse testing for new cells without lithium plating and for aged cells with lithium plating. For comparison, the cell mass before the safety tests was (45.35 ± 0.13) g.

temperatures than new cells. Overdischarge showed similar T_{max} values for new and aged cells. During the overcurrent tests, all aged cells reached higher temperatures than new cells. In particular two of the aged cells with lithium plating even reached TR with significantly higher maximum temperatures. It should also be noted that the overcurrent tests of the aged cells stopped after one discharge due to CID triggering and TR, which is in strong contrast to the new cells which could still perform 100 cycles. During the nail penetration testing, all new cells and aged cells achieved comparable average maximum temperatures.

Comparing the results of the different safety test methods, the highest T_{max} values were obtained for nail penetration and ARC. In contrast, lower T_{max} values were observed for the electrical abuse tests (overcharge, overdischarge, and overcurrent). The reasons for the higher T_{max} values in nail penetration and ARC experiments are most likely that the harsh conditions—short circuits and the quasi-adiabatic conditions, respectively—lead to more severe TR events.

Essl et al. compared new and aged 60 Ah pouch cells (graphite‖ NMC) in overtemperature tests.[97] The authors found similar or lower T_{max} values for cells cycled at $-10\,°C$, however, these cells had a rest time after cycling allowing the cells to recover.[97] We had observed a similar recovery effect for same safety aspects for 18650 cells with lithium plating after a rest time in ARC experiments.[26] This partial recovery effect is connected to re-intercalation of lithium metal into graphite[25,26,34,98,99] and Si/graphite[19,22] anodes and reaction with electrolyte[14,25] during the rest time.

The lower the cell mass after a safety test, the higher the degree of destruction. Cells masses after nail penetration, overdischarge, overcurrent, and overcharge tests are shown in Fig. 10b. We note that determination of the cell masses was very difficult after the ARC tests, therefore the values for ARC are not contained in this plot.

The cell masses after the tests of new cells without lithium plating and aged cells with lithium plating were mostly similar for each safety test method, with a few exceptions. For overcurrent cycling, the cell masses showed slightly reduced values for the aged cells with lithium plating, although two of these cells experienced a TR (see Fig. 8a). The cells which underwent TR produced a large amount of smoke, but no visible fire and no ejection of the jelly roll. In case of the overcharge tests, two of the aged cells showed a similar mass after the test as all new cells, while one aged cell showed the lowest mass after all the tests. This is the same cell which had a higher maximum temperature during TR (black curve in Fig. 6a).
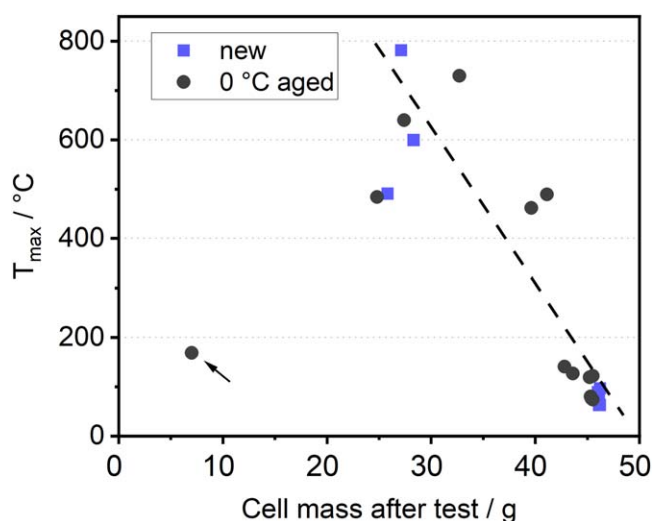

Figure 11. Correlation between maximum temperature during TR and cell mass after safety tests. The arrow marks the result of the overcharge test with the lowest cell mass of all tests. The dashed line is drawn to guide the eye. For comparison, the cell mass before the safety tests was (45.35 ± 0.13) g.

Comparing the different safety test methods, a lower average mass after the tests was found for the nail penetration tests, while the highest mass loss was found for only one of the overcharge tests. All other overcharge tests, as well as all overdischarge and overcurrent tests, showed minor mass losses.

Figure 11 shows a correlation of the maximum temperatures during TR and the cell masses after the different types of tests with new and aged cells. All data points except the overcharge test with the lowest cell mass (arrow in Fig. 11, black curve in Fig. 6a) follow a trend (see dashed line to guide the eye in Fig. 11). In general, Fig. 11 shows that a higher T_{max} during TR most likely leads to higher mass losses of the cells, causing a more severe safety event.

A well-established approach to battery safety assessment involves the use of hazard levels as proposed by the European Council for Automotive Research and Development (EUCAR).[50] The EUCAR hazard levels were determined based on the events observed in each cell during the corresponding safety tests, and they are represented in Fig. 12. Note that for larger cells or battery packs, the safety incidents may be even more severe, but here we
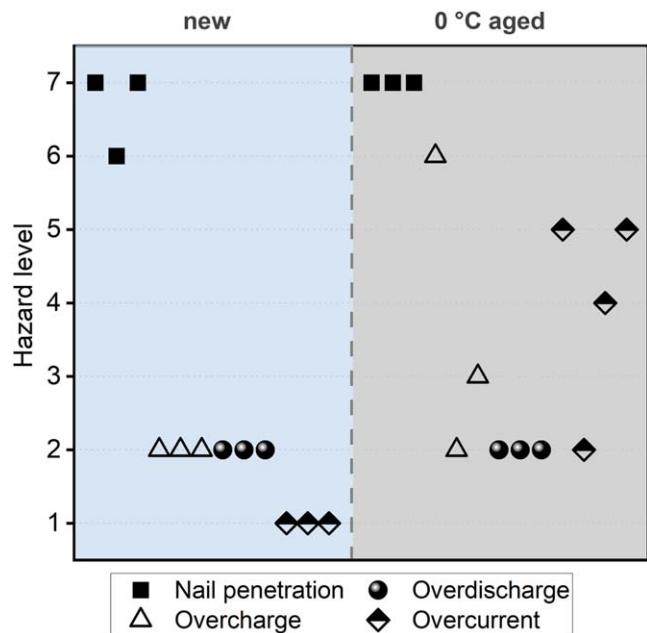
Figure 12. Comparison of EUCAR hazard levels during nail penetration, overcharge, overdischarge, and overcurrent tests for new cells without lithium plating and for aged cells with lithium plating.
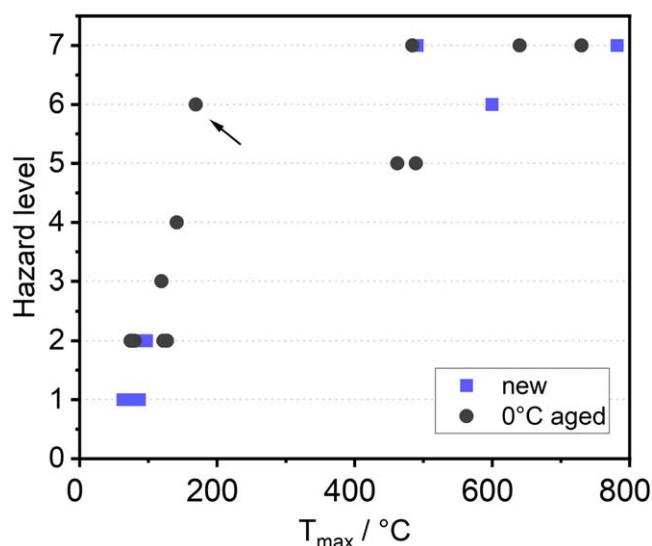

Figure 13. Correlation between EUCAR hazard level and T_{max} during TR. The arrow marks the result of the overcharge test with the lowest cell mass of all tests.

have used the full scale of EUCAR hazard levels to evaluate 18650 cells. As direct observations of the cell events during the ARC tests were not possible, they were excluded from this analysis.

Throughout the overcharge tests, CIDs were activated in both new cells and aged cells. Notably, two of the aged cells exhibited leakage and cell explosion, respectively. In sharp contrast, new cells and one aged cell showed no visual events in the overcharge tests. Overdischarge and overcurrent tests induced the activation of CIDs only in aged cells. During overcurrent tests, leakage was observed in one aged cell, and a more pronounced venting was observed in the case of other two aged cells which also had a higher mass loss (see Fig. 10b). During overdischarge and overcurrent, no further visual events were observed for new cells. However, despite the absence of a PTC within the tested commercial 18650-type LIB cells observed by Post-Mortem analysis, an assigned hazard level of one was

deemed appropriate due to the temperatures reached above 60 °C in the new cells. Across all safety tests, the aged cells with lithium plating had consistently higher hazard levels compared to new cells without lithium plating. This highlights the potential hazards associated with lithium plating in LIBs.

Hazard levels of aged cells are difficult to discuss in context of literature for different safety test methods, since, to best of our knowledge, no datasets comparable to the one presented herein are available so far. However, we had shown for two different types of commercial cylindrical cells[11,26] and for lab pouch cells,[51] that the degree of destruction can be higher for cells with lithium plating after ARC tests.

Comparing the different safety test methods, the highest EUCAR hazard levels were obtained for the nail penetration and overcurrent tests, as well as for one of the overcharge tests. This is in accordance with the higher maximum temperatures and lower cell masses after the safety tests for the same cells.

Figure 13 shows that higher T_{max} values during TR likely lead to increased EUCAR hazard levels. The observed trend might be regarded as linear until hazard level 4 and runs into a saturation for higher hazard levels. We note that the cell from the overcharge test, which showed the lowest cell mass after of all tests (arrow in Figs. 11 and 13, black curve in Fig. 6a) also follows this trend.

Clearly, measures must be implemented to mitigate or entirely prevent lithium plating on the anodes of LIBs. Preventive strategies against lithium plating include charging protocols that avoid negative anode potentials,[16,51,100,101] increased temperatures during charging,[5,7,8,10,13,16,63,100,102,103] reduced anode coating thicknesses,[8,19,63] and the use of laser-structured anodes with reduced tortuosity.[104] We have recently published workflows using validated methods to identify lithium depositions in LIB cells which might be helpful in this regard.[35]

Conclusions

We have comprehensively explored the safety behavior of 29 commercial LIB cells with and without lithium plating on the graphite anodes. Various mechanical, electrical, and thermal abuse test methods have been applied. Post-Mortem analysis and electro-chemical data showed that the cells aged by cycling at 0 °C show lithium plating as main ageing mechanism, whereas new (non-aged) cells and cells aged at 45 °C did not show lithium plating.

Safety tests in this work focus on the comparison of new cells without lithium plating and aged cells with lithium plating. Comparative analysis of the test results between new and aged cells provided valuable insights into the safety behavior. Our results show that lithium plating is a severe aging mechanism, which does not only lead to fast capacity decrease, but also to a decreased safety behavior in different safety test methods.

The present study revealed the following trends:

• Comparing new cells without lithium plating with aged cells with lithium plating, increased EUCAR hazard levels were found in overdischarge, overcharge, and overcurrent experiments. The increase was particularly pronounced for overcurrent cycling of aged cells with lithium plating. The hazard levels were similarly high for new and aged cells in nail penetration tests.

• In comparison with new cells without lithium plating, aged cells with lithium plating showed a tendency of higher maximum temperatures during the safety tests. A slight tendency of higher T_{max} was found for ARC, overcharge, and overdischarge. For overcurrent cycling, two out of four tested cells went into TR in the first discharge step and showed strongly increased T_{max} values with respect to the new cells. The maximum temperatures of new and aged cells were similarly high in nail penetration tests.

• The observed tendency to increased maximum temperatures is connected to exothermic reactions of deposited lithium metal with electrolyte. We stress that the TR events presented herein are not due to short circuits by lithium dendrites.

- In an overall evaluation, the maximum temperature showed correlations with the EUCAR hazard levels and with the cell mass after test. Therefore, also the reactivity and the exothermic reactions of the lithium depositions are connected to these safety relevant parameters.
- The different types of safety tests lead to different results regarding maximum temperature, mass loss, and hazard level. Among the tested methods, the nail penetration tests lead to the most severe results for the tested cell type. Furthermore, some safety test methods emphasize the differences between new and aged cells more than others.

The potential hazard associated with lithium plating in LIBs is underscored by the results of our comprehensive safety assessment. We note that the applied cyclic aging procedure at 0 °C accelerates aging and leads to comparably large amounts of deposited lithium on the anode. Although the applied conditions are within the specification given by the cell manufacturer, such high amounts of plated lithium might not be representative for battery aging in applications. However, the critical amount of deposited lithium to significantly influence the results of different types of safety tests is not known so far. Nevertheless, during operation of LIBs in applications, conditions leading to lithium deposition, i.e. critical combinations of low temperatures, high charging C-rates, and high SOCs should be avoided for safer use in second-life applications. It might also be an option to closely monitor indicators for lithium plating in first-life applications. It is also important to detect lithium plating in representative cells from LIB systems before reuse in second-life applications. We have recently published workflows using validated methods for detecting and preventing lithium plating as well as identifying operating conditions where lithium plating does not occur.[35]

In addition to the results shown for cells with lithium plating, more knowledge must be gained on the safety behavior of aged cells with aging mechanisms other than lithium plating, for cells aged in applications, as well as for aged modules, heating behavior of aged cells with increased impedance, different amounts of deposited lithium, gas evolution, electrical and mechanical response, as well as larger test statistics. This is part 1 of a paper series; part 2 deals with safety tests of aged cells without the aging mechanism of lithium plating.

ORCID

Gabriela G. Gerosa https://orcid.org/0000-0001-8701-965X
Max Feinauer https://orcid.org/0000-0003-2483-8257
Christin Hogrefe https://orcid.org/0000-0001-9952-8507
Katharina Bischof https://orcid.org/0009-0004-0321-3252
Margret Wohlfahrt-Mehrens https://orcid.org/0000-0002-5118-5215
Markus Hölzle https://orcid.org/0009-0004-8278-1089
Thomas Waldmann https://orcid.org/0000-0003-3761-1668

References

1. K. Hantanasirisakul and M. Sawangphruk, *Global Challenges (Hoboken, NJ)*, **7**, 2200212 (2023).
2. N. O. Bonsu, *J. Clean. Prod.*, **256**, 120659 (2020).
3. A. Barré, B. Deguilhem, S. Grolleau, M. Gérard, F. Suard, and D. Riu, *J. Power Sources*, **241**, 680 (2013).
4. T. Waldmann et al., *J. Electrochem. Soc.*, **163**, A2149 (2016).
5. T. Waldmann, M. Wilka, M. Kasper, M. Fleischhammer, and M. Wohlfahrt-Mehrens, *J. Power Sources*, **262**, 129 (2014).
6. J. Zhu et al., "End-of-life or second-life options for retired electric vehicle batteries." *Cell Reports Physical Science*, **2**, 100537 (2021).
7. G. Kucinskis, M. Bozorgchenani, M. Feinauer, M. Kasper, M. Wohlfahrt-Mehrens, and T. Waldmann, *J. Power Sources*, **549**, 232129 (2022).
8. M. Bozorgchenani, G. Kucinskis, M. Wohlfahrt-Mehrens, and T. Waldmann, *J. Electrochem. Soc.*, **169**, 30509 (2022).
9. M. Feinauer, A. A. Abd-El-Latif, P. Sichler, A. A. Regalado, M. Wohlfahrt-Mehrens, and T. Waldmann, *J. Power Sources*, **570**, 233046 (2023).
10. M. Feinauer, M. Wohlfahrt-Mehrens, M. Hölzle, and T. Waldmann, *J. Power Sources*, **594**, 233948 (2024).
11. M. Fleischhammer, T. Waldmann, G. Bisle, B-I. Hogg, and M. Wohlfahrt-Mehrens, *J. Power Sources*, **274**, 432 (2015).
12. J. C. Burns, D. A. Stevens, and J. R. Dahn, *J. Electrochem. Soc.*, **162**, A959 (2015).
13. T. Waldmann, B-I. Hogg, and M. Wohlfahrt-Mehrens, *J. Power Sources*, **384**, 107 (2018).
14. D. Stottmeister and A. Groß, *Batteries & Supercaps*, **6** (2023).
15. S. Hein and A. Latz, *Electrochim. Acta*, **201**, 354 (2016).
16. T. Waldmann, B-I. Hogg, M. Kasper, S. Grolleau, C. G. Couceiro, K. Trad, B. P. Matadi, and M. Wohlfahrt-Mehrens, *J. Electrochem. Soc.*, **163**, A1232 (2016).
17. M. Boerner, A. Friesen, M. Gruetzke, Y. P. Stenzel, G. Brunklaus, J. Haetge, S. Nowak, F. M. Schappacher, and M. Winter, *J. Power Sources*, **342**, 382 (2017).
18. M. Flügel, K. Richter, M. Wohlfahrt-Mehrens, and T. Waldmann, *J. Electrochem. Soc.*, **169**, 50533 (2022).
19. M. Flügel, M. Bolsinger, M. Marinaro, V. Knoblauch, M. Hölzle, M. Wohlfahrt-Mehrens, and T. Waldmann, *J. Electrochem. Soc.*, **170**, 60536 (2023).
20. P. Kuntz, O. Raccurt, P. Azais, K. Richter, T. Waldmann, M. Wohlfahrt-Mehrens, M. Bardet, A. Buzlukov, and S. Genies, *Batteries*, **7** (2021).
21. K. Richter, T. Waldmann, M. Kasper, C. Pfeifer, M. Memm, P. Axmann, and M. Wohlfahrt-Mehrens, *J. Phys. Chem. C*, **123**, 18795 (2019).
22. K. Richter, T. Waldmann, N. Paul, N. Jobst, R-G. Scurtu, M. Hofmann, R. Gilles, and M. Wohlfahrt-Mehrens, *ChemSusChem*, **13**, 529 (2020).
23. M. Petzl and M. A. Danzer, *J. Power Sources*, **254**, 80 (2014).
24. T. Waldmann, M. Kasper, and M. Wohlfahrt-Mehrens, *Electrochim. Acta*, **178**, 525 (2015).
25. T. Waldmann, J. B. Quinn, K. Richter, M. Kasper, A. Tost, A. Klein, and M. Wohlfahrt-Mehrens, *J. Electrochem. Soc.*, **164**, A3154 (2017).
26. T. Waldmann and M. Wohlfahrt-Mehrens, *Electrochim. Acta*, **230**, 454 (2017).
27. A. A. Abd-El-Latif, P. Sichler, M. Kasper, T. Waldmann, and M. Wohlfahrt-Mehrens, *Batteries & Supercaps*, **4**, 1135 (2021).
28. B. P. Matadi et al., *J. Electrochem. Soc.*, **164**, A1089 (2017).
29. K. Jalkanen, J. Karppinen, L. Skogström, T. Laurila, M. Nisula, and K. Vuorilehto, *Appl. Energy*, **154**, 160 (2015).
30. K. Iturrondobeitia, F. Aguesse, S. Genies, T. Waldmann, M. Kasper, N. Ghanbari, M. Wohlfahrt-Mehrens, and E. Bekaert, *J. Phys. Chem. C*, **121**, 21865 (2017).
31. D. Anseán, M. Dubarry, A. Devie, B. Y. Liaw, V. M. García, J. C. Viera, and M. González, *J. Power Sources*, **356**, 36 (2017).
32. M. Dubarry, C. Truchot, B. Y. Liaw, K. Gering, S. Sazhin, D. Jamison, and C. Michelbacher, *J. Electrochem. Soc.*, **160**, A191 (2013).
33. M. Ecker, P. Shafiei Sabet, and D. U. Sauer, *Appl. Energy*, **206**, 934 (2017).
34. V. Zinth, C. von Lüders, M. Hofmann, J. Hattendorff, I. Buchberger, S. Erhard, J. Rebelo-Kornmeier, A. Jossen, and R. Gilles, *J. Power Sources*, **271**, 152 (2014).
35. T. Waldmann et al., *J. Electrochem. Soc.*, **171**, 70526 (2024).
36. S. Ohneseit, P. Finster, C. Floras, N. Lubenau, N. Uhlmann, H. J. Seifert, and C. Ziebert, *Batteries*, **9**, 237 (2023).
37. C. Essl, A. W. Golubkov, and A. Fuchs, *J. Electrochem. Soc.*, **167**, 130542 (2020).
38. N. Böttcher, S. Dayani, H. Markötter, A. Bau, M. Setzchen, A. Schmidt, J. Kowal, and J. Krug von Nidda, *Energy Technol.*, **12**, 2301379 (2024).
39. B. Bausch, S. Frankl, D. Becher, F. Menz, T. Baier, M. Bauer, O. Böse, and M. Hölzle, *Journal of Energy Storage*, **61**, 106841 (2023).
40. K. M. Abraham, *J. Electrochem. Soc.*, **170**, 110508 (2023).
41. G. Zhang, X. Wei, X. Tang, J. Zhu, S. Chen, and H. Dai, *Renew. Sustain. Energy Rev.*, **141**, 110790 (2021).
42. Y. Preger, L. Torres-Castro, T. Rauhala, and J. Jeevarajan, *J. Electrochem. Soc.*, **169**, 30507 (2022).
43. C. Fear, D. Juarez-Robles, J. A. Jeevarajan, and P. P. Mukherjee, *J. Electrochem. Soc.*, **165**, A1639 (2018).
44. S. Yayathi, W. Walker, D. Doughty, and H. Ardebili, *J. Power Sources*, **329**, 197 (2016).
45. J. Lamb, L. Torres-Castro, J. C. Hewson, R. C. Shurtz, and Y. Preger, *J. Electrochem. Soc.*, **168** (2021).
46. M. N. Richard and J. R. Dahn, *J. Electrochem. Soc.*, **146**, 2068 (1999).
47. E. Roth and D. H. Doughty, *J. Power Sources*, **128**, 308 (2004).
48. Dan Doughty and E. P. Roth, *Electrochem. Soc. Interface*, **21**, 37 (2012).
49. M. Feinauer, M. Hölzle, and T. Waldmann, *Electrochem. Soc. Interface*, **33**, 51 (2024).
50. C. N. Ashtiani, *ECS Trans.*, **11**, 1 (2008).
51. B.-I. Hogg, T. Waldmann, and M. Wohlfahrt-Mehrens, *J. Electrochem. Soc.*, **167**, 90525 (2020).
52. H. Kondou, J. Kim, and H. Watanabe, *Electrochemistry*, **85**, 647 (2017).

53. J. Liu, Z. Wang, J. Bai, T. Gao, and N. Mao, *Appl. Therm. Eng.*, **212**, 118565 (2022).
54. M. Feinauer, A. A. Abd-El-Latif, P. Sichler, M. Wohlfahrt-Mehrens, M. Hölzle, and T. Waldmann, *J. Electrochem. Soc.*, **171**, 110524 (2024).
55. J. B. Quinn, T. Waldmann, K. Richter, M. Kasper, and M. Wohlfahrt-Mehrens, *J. Electrochem. Soc.*, **165**, A3284 (2018).
56. I. Pivarníková, M. Flügel, N. Paul, A. Cannavo, G. Ceccio, J. Vacík, P. Müller-Buschbaum, M. Wohlfahrt-Mehrens, R. Gilles, and T. Waldmann, *J. Power Sources*, **594**, 233972 (2024).
57. B. Bitzer and A. Gruhle, *J. Power Sources*, **262**, 297 (2014).
58. S. Gorse, B. Kugler, T. Samtleben, T. Waldmann, M. Wohlfahrt-Mehrens, G. Schneider, and V. Knoblauch, *Practical Metallography*, **51**, 829 (2014).
59. T. Waldmann, S. Gorse, T. Samtleben, G. Schneider, V. Knoblauch, and M. Wohlfahrt-Mehrens, *J. Electrochem. Soc.*, **161**, A1742 (2014).
60. C. Weisenberger, B. Meir, S. Röhler, D. K. Harrison, and V. Knoblauch, *Electrochim. Acta*, **379**, 138145 (2021).
61. X. Fleury, M. H. Noh, S. Geniès, P. X. Thivel, C. Lefrou, and Y. Bultel, *Journal of Energy Storage*, **16**, 21 (2018).
62. N. Ghanbari, T. Waldmann, M. Kasper, P. Axmann, and M. Wohlfahrt-Mehrens, *J. Phys. Chem. C*, **120**, 22225 (2016).
63. X-G. Yang and C-Y. Wang, *J. Power Sources*, **402**, 489 (2018).
64. J. C. Burns, A. Kassam, N. N. Sinha, L. E. Downie, L. Solnickova, B. M. Way, and J. R. Dahn, *J. Electrochem. Soc.*, **160**, A1451 (2013).
65. N. Ghanbari, T. Waldmann, M. Kasper, P. Axmann, and M. Wohlfahrt-Mehrens, *ECS Electrochem. Lett.*, **4**, A100 (2015).
66. R. V. Bugga and M. C. Smart, *ECS Trans.*, **25**, 241 (2009).
67. C. Hogrefe, T. Waldmann, M. Hölzle, and M. Wohlfahrt-Mehrens, *J. Power Sources*, **556**, 232391 (2023).
68. Y. Chen, *Ionics*, **28**, 495 (2022).
69. D. Ren, X. Feng, L. Lu, M. Ouyang, S. Zheng, J. Li, and X. He, *J. Power Sources*, **364**, 328 (2017).
70. J. E. Harlow et al., *J. Electrochem. Soc.*, **166**, A3031 (2019).
71. W. Mei, L. Zhang, J. Sun, and Q. Wang, *Energy Storage Mater.*, **32**, 91 (2020).
72. T. Ohsaki, T. Kishi, T. Kuboki, N. Takami, N. Shimura, Y. Sato, M. Sekino, and A. Satoh, *J. Power Sources*, **146**, 97 (2005).
73. Q. Yuan, F. Zhao, W. Wang, Y. Zhao, Z. Liang, and D. Yan, *Electrochim. Acta*, **178**, 682 (2015).
74. Y. Luo, C. Sang, K. Le, H. Chen, H. Li, and X. Ai, *J. Energy Chem.*, **94**, 181 (2024).
75. H. Mao and U. Von Sacken, *Aromatic monomer gassing agents for protecting non-aqueous lithium batteries against overcharge*, US5776627A (1998), 7.
76. S. S. Zhang, *J. Power Sources*, **164**, 351 (2007).
77. T. Waldmann and M. Wohlfahrt-Mehrens, *ECS Electrochem. Lett.*, **4**, A1 (2015).
78. T. Waldmann, G. Geramifard, and M. Wohlfahrt-Mehrens, *Journal of Energy Storage*, **5**, 163 (2016).
79. T. Waldmann, R-G. Scurtu, D. Brandle, and M. Wohlfahrt-Mehrens, *Energy Technol.*, 2200583 (2022).
80. X. Zhang, *Electrochim. Acta*, **56**, 1246 (2011).
81. J. Sturm, A. Frank, A. Rheinfeld, S. V. Erhard, and A. Jossen, *J. Electrochem. Soc.*, **167**, 130505 (2020).
82. T. Waldmann, G. Bisle, B-I. Hogg, S. Stumpp, M. A. Danzer, M. Kasper, P. Axmann, and M. Wohlfahrt-Mehrens, *J. Electrochem. Soc.*, **162**, A921 (2015).
83. M. Flügel, M. Kasper, C. Pfeifer, M. Wohlfahrt-Mehrens, and T. Waldmann, *J. Electrochem. Soc.*, **168**, 20506 (2021).
84. R. Guo, L. Lu, M. Ouyang, and X. Feng, *Sci Rep.*, **6**, 30248 (2016).
85. M. Flügel, T. Waldmann, M. Kasper, and M. Wohlfahrt-Mehrens, *A European Journal of Chemical Physics and Physical Chemistry, Chem. Phys. Chem.*, **21**, 2047 (2020).
86. J. Kasnatscheew, M. Börner, B. Streipert, P. Meister, R. Wagner, I. Cekic Laskovic, and M. Winter, *J. Power Sources*, **362**, 278 (2017).
87. S. Dayani, H. Markötter, J. Krug von Nidda, A. Schmidt, and G. Bruno, *Adv. Mater. Technol.*, **9**, 2301246 (2023).
88. B. Liu, Y. Jia, C. Yuan, L. Wang, X. Gao, S. Yin, and J. Xu, *Energy Storage Mater.*, **24**, 85 (2020).
89. A. Friesen, F. Horsthemke, X. Mönnighoff, G. Brunklaus, R. Krafft, M. Börner, T. Risthaus, M. Winter, and F. M. Schappacher, *J. Power Sources*, **334**, 1 (2016).
90. Y. Liu, Y. Xia, and Q. Zhou, *Energy Storage Mater.*, **40**, 268 (2021).
91. L. Willenberg, P. Dechent, G. Fuchs, M. Teuber, M. Eckert, M. Graff, N. Kürten, D. U. Sauer, and E. Figgemeier, *J. Electrochem. Soc.*, **167**, 120502 (2020).
92. M. Bauer, M. Wachtler, H. Stöwe, J. V. Persson, and M. A. Danzer, *J. Power Sources*, **317**, 93 (2016).
93. B. Rieger, S. F. Schuster, S. V. Erhard, P. J. Osswald, A. Rheinfeld, C. Willmann, and A. Jossen, *Journal of Energy Storage*, **8**, 1 (2016).
94. J. Vetter, P. Novák, M. R. Wagner, C. Veit, K-C. Möller, J. O. Besenhard, M. Winter, M. Wohlfahrt-Mehrens, C. Vogler, and A. Hammouche, *J. Power Sources*, **147**, 269 (2005).
95. J. Self, C. P. Aiken, R. Petibon, and J. R. Dahn, *J. Electrochem. Soc.*, **162**, A796 (2015).
96. K. Kumai, H. Miyashiro, Y. Kobayashi, K. Takei, and R. Ishikawa, *J. Power Sources*, **81–82**, 715 (1999).
97. C. Essl, A. W. Golubkov, and A. Fuchs, *Batteries-Basel*, **7**, 23 (2021).
98. C. Uhlmann, J. Illig, M. Ender, R. Schuster, and E. Ivers-Tiffée, *J. Power Sources*, **279**, 428 (2015).
99. C. Hogrefe, S. Hein, T. Waldmann, T. Danner, K. Richter, A. Latz, and M. Wohlfahrt-Mehrens, *J. Electrochem. Soc.*, **167** (2020).
100. J. Remmlinger, S. Tippmann, M. Buchholz, and K. Dietmayer, *J. Power Sources*, **254**, 268 (2014).
101. C. Hogrefe, M. Hölzle, M. Wohlfahrt-Mehrens, and T. Waldmann, *J. Electrochem. Soc.*, **170**, 110535 (2023).
102. X-G. Yang, T. Liu, Y. Gao, S. Ge, Y. Leng, D. Wang, and C-Y. Wang, *Joule*, **3**, 3002 (2019).
103. S. Tippmann, D. Walper, L. Balboa, B. Spier, and W. G. Bessler, *J. Power Sources*, **252**, 305 (2014).
104. K-H. Chen et al., *J. Power Sources*, **471**, 228475 (2020).